VERIZONA PUBLISHER
Publishing Your Ideas

www.verizonaonlinepublishing.com
Special Issue

Material Science and Engineering with Advanced Research

Vacuum Arc Melting Processed Fe-Al Matrix Based Intermetallic Composites, Reinforced with VC Phases: Assessment of Microstructure, Sliding Wear and Aqueous Corrosion Response

E Karapanou, AG Lekatou, AK Sfikas, E Georgatis, K Lentzaris and AE Karantzalis*

Laboratory of Applied Metallurgy, Department of Materials Science & Engineering, University of Ioannina, 45110 Ioannina, Hellas

***Corresponding author:** AE Karantzalis, Laboratory of Applied Metallurgy, Department of Materials Science & Engineering, University of Ioannina, 45110 Ioannina, Hellas, Greece; Tel: (+30) 2651009026; Fax: (+30) 2651009082; E mail: akarantz@cc.uoi.gr

Article Type: Research, **Submission Date**: 03 February 2017, **Accepted Date:** 10 February 2017, **Published Date:** 11 May 2017.

Citation: E Karapanou, AG Lekatou, AK Sfikas, E Georgatis, K Lentzaris and AE Karantzalis (2017) Vacuum Arc Melting Processed Fe-Al Matrix Based Intermetallic Composites, Reinforced with VC Phases: Assessment of Microstructure, Sliding Wear and Aqueous Corrosion Response. Mater. Sci. Eng. Adv. Res Special Issue: 1-6. doi: https://doi.org/10.24218/msear.2017.1S.

Abstract

Fe-Al based intermetallic matrix composites reinforced with VC phases by a dissolution- re-precipitation method where successfully produced through the utilisation of vacuum arc melting process. The microstructure of the produced materials was examined using optical microscopy and SEM-EDX analysis revealing various modifications of the precursor reinforcing phases.The wear properties of the composites were examined by dry sliding wear against a6Cr steel ball as counter-face, at 10cm/s, with load 2N externally applied load and an overall sliding distance of 2400m. The worn surfaces and the produced debris were examined by SEM-EDX and an effort to correlate the wear response of the produced materials with the intermetallic matrix and the reinforcing phase characteristics was attempted. In a similar manner,in order to ascertain the corrosion response of the produced materials, cyclic polarization measurements were conducted in a 1N H_2SO_4 aqueous solution. The corroded surfaces were also examined by SEM-EDX and possible corrosion mechanisms and phenomena are proposed based on the microstructural features.

Keywords: Fe-Alintermetallics, Composites, Erosion, Sliding wear, Aqueous corrosion.

Introduction

It has been almost two decades since it was realized that iron aluminides - Fe_3Al andFeAl – comprise an interesting class of intermetallic materials as potential candidates for the substitution of stainless steels in structural applications at both moderate andhigh temperatures due to attractive properties such as good wear [1-8] and excellentcorrosion resistance [9] even at high temperatures, ease of fabrication, low productioncost, reduced density compared to other ferrous alloys and reasonable strength up to 550°C. The main drawbacks for the commercialization of such materials are their poor room temperature ductility and strength decrease above 550°C [10]. Researchers have been attempting to solve these problems either by using non-conventional manufacturing/processing routes or/and by elemental alloying additions [8-10].

Iron aluminides have been considered the material for a variety of anti-wear applications; they could replace conventional wear resistance cobalt-base alloys andiron-based alloys containing chromium and manganese. Extrinsic parameters related to the wear tests conditions, alloying with other elements and precise control of the Fe to Al ratio have been considered as major factors for improved wear resistance of the Fe-Al intermetallics. Within this frame of improving these materials wear resistance, the introduction of hard ceramic particles havealso been proposed as a very effective alternative [11-22].

The excellent corrosion of iron aluminides has also attracted significant research interest. The characteristics of the corrosive environment, the compositional and microstructural features of the intermetallic phase and the appropriate actions to control the nature the extent and the stability of the various oxide and other passivation surface films, are some of the key factor while assessing the corrosion response of this class of materials [23-24].

Experimental Procedure

Appropriate amounts of Fe (electrolytic, 99,9% purity), Al (commercial purity 99,7%) and VC powder (<44μm) were weighted, mixed, melted in arc melting furnace using Ar as protective atmosphere and W electrode at 120A current to produce monolithic Fe-22at.%Al intermetallic phase matrix

and 1, 5 and 10wt% VC composites with Fe-22at.%Al matrix. Specimens were metallographically prepared and examined under optical microscope (Leica 4000DM) and SEM-EDX (Jeol 6510LV, x-Act EDX system by Oxford Instruments) in order to assess their microstructural features.

Sliding wear experiments were conducted using CSM ball – on disk tribometer, using a 6Cr steel ball of 6mm diameter as counterbody at 10cm/s sliding speed, 2N externally applied load, 45Hz acquisition rate, 6mm wear track diameter and 2400 m as an overall sliding distance. The tests were interrupted every 200m for specimen weighting and mass loss recording.

Aqueous corrosion experiments were conducted in properly prepared samples using a Gill AC galvanostat by ACM Instruments, within a 1N H_2SO_4 solution, using an Ag/ AgCl/ 3.5KCl reference electrode and a Pt secondary electrode. The experiments were conducted keeping the solution pH at 7, at scanning rate of 10mV/min within the range of -1000 to 2000 mV after having ascertained the rest potential for 2h. Chronoamperometry tests were also conducted at various potentials (0, 500 and 1000mV) for 2h.

Results and Discussion

Microstructural assessment

Figure 1 presents a panoramic view of the microstructure of both the monolithic intermetallic matrix and the composite materials produced in the present effort. It can be observed that in the case of the pure matrix and the 1% reinforced material the microstructure does not reveal any distinguishing morphology with the exemption of some porosity especially in the case of the monolithic alloy. In the 5% and 10% reinforced composites, it appears that a second phase is formed at the grain boundaries resembling to a eutectic microconstituent being more extended in the case of the 10% reinforced material.

A closer examination with EDX analysis of this eutectic area in the case of the 10% reinforced material, is shown in Figure 2. It can be observed from the elemental mapping analysis that this eutectic compound show high concentration of V and C and as such it can be postulated that it may consist of mainly V based carbide phases.

Table 1 shows the hardness values of the different materials. It can be observed that the 1% shows an increased hardness value

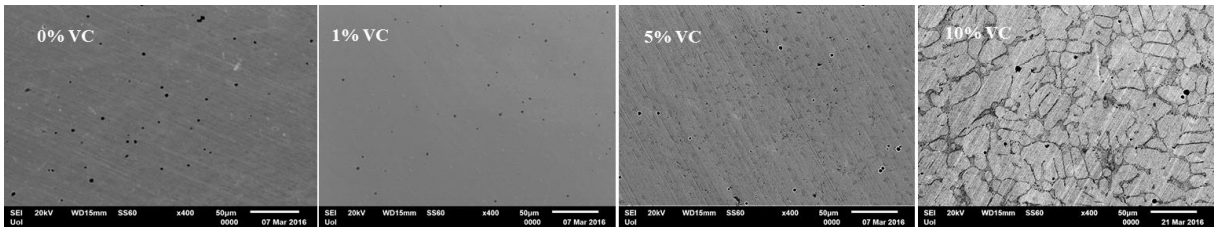

Figure 1: Panoramic view of the microstructures of the produced materials

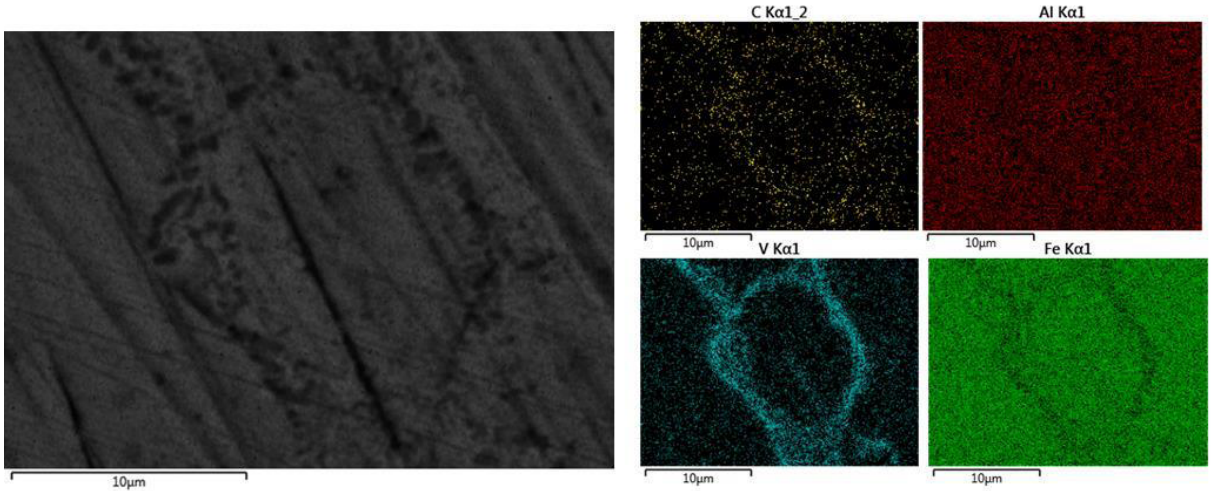

Figure 2: Elemental mapping of the eutectic like compound in the case of 10% reinforced material

Table 1: Hardness Values of the Different Materials Produced in the Present Effort

Material	Hardness(Rockwell HRC)
Monolithic	26 ± 2
1 wt% VC	29 ± 3
5 wt% VC	32 ± 1
10 wt%VC	32 ± 1

compared to that of the monolithic alloy, which is most likely associated with the dilution of V and C in the Fe-Al lattice resulting in solid solution strengthening. The hardness increase for 5 and 10% is not considerable, however, despite the presence of eutectic phases and an analysis based on binary phases diagrams, used in order to explain this discrepancy. The relative ratios for each pair of elements were calculated for the initial molten state and an effort was undertaken in order to predict based on the binary phase diagrams a possible sequence of solid phases being precipitates during cooling. The results of this approach are presented in Table 2.

Based on the data of Table 2 it can be postulated that in the case of the 1% material potential carbide or V aluminide phases may form upon solidification, yet the V and C low concentration may either restrict their formation or make it very limited and undetected by SEM-EDS techniques. In the case of 5% system eutectic V based carbide phases form (observed at the grain boundaries) at the early stages of solidification probably followed by a limited formation of Al_4C_3. The situation becomes more complex in the case of 10% reinforced material. A possible solid phase precipitation sequence may be VC carbides eutectic, Al_4C_3 Al_8V_5 finished by the A2 formation. Such sequence, however, may significantly deplete the liquid phase especially from Al prior to the formation of A2, shifting the Fe-Al composition far beyond the original proportions. Such alteration may significantly reduce the solid solution strengthening effect in the matrix alloy, explaining thus the low hardness retaining levels.

Sliding Wear Resistance

Figure 3 presents the sliding wear results of the different materials showing the wear rates, a panoramic view of the wear tracks and a characteristic EDS analysis on the selected area of the 5% material showing the formation of oxide phases.

The data from Figure 3 clearly indicates that the increase of the VC addition leads to a reduction of the wear rates. This postulation is in agreement with the classic theory of Archard [25] according to which an increase on the hardness (and the brittle character) of the material leads to improvement in the wear resistance. The formation of the oxide phases accounts from both the degradation phenomena as cracks can be initiated and propagated through the oxide film leading to material removal and a lubricant action at prolonged sliding distances retarding the material loss especially if the oxide phases are rich in Fe oxides [26]. Similar conclusions have also been drawn in other experimental works [27].

Aqueous Corrosion Response

Figure 4 shows the cyclic poententiodynamic curves of the different materials and Figure 5 the forward parts of them superimposed for comparison reasons. In both Figures the major conclusions are included.

Figure 6 shows the results of the chronoamperometry tests and their main conclusions in conjunction with cyclic polarization, concerning the aqueous corrosion behavior of the materials, are shown in Table 3. All data was received by appropriate SEM – EDX analysis, which is not quoted for space limitation reasons.

Conclusions

1. Monolithic Fe-Al alloys 1, 5 and 10 wt.% VC based Fe-Al composites were successfully produced by VAM process.

Table 2: Temperatures of Potential Solid Phase Formation for Each Pair of Elements DuringCooling According to the Corresponding Binary Phase Diagrams and the Elemental Ratios for Each System

Material	Fe / Al	Fe / V	Fe / C	V / Al	V / C	Al / C
Fe - 22%at.Al	1500°C:a-Fe 850°C:A2FeAl 500-550°C: DO_3 Fe_3Al	-	-	-	-	-
Fe - 22%at.Al – 1wt% VC	1500°C:a-Fe 850°C:A2FeAl 500-550°C: DO_3 Fe_3Al	1580°C:a-Fe 1360°C:γ-Fe 1000°C:a-Fe	1540°C: δ-Fe	1600°C: Al_3V	2600°C: EutecticVC+ V - carbide	1850°C: Al_4C_3
Fe - 22%at.Al – 5wt% VC	1500°C:a-Fe 850°C:A2FeAl 500-550°C: DO_3 Fe_3Al	1500°C:a-Fe	1480°C: γ-Fe	1400°C: Al_8V_5 1360°C: Al_3V	2600°C: EutecticVC+ V – carbide	2200°C: Al_4C_3
Fe - 22%at.Al – 10wt% VC	1500°C:a-Fe 850°C:A2FeAl 500-550°C: DO_3 Fe_3Al	1470-1480°C: a-Fe	1300°C: γ-Fe	1650°C: Al_8V_5 1360°C: Al_3V	2600°C: EutecticVC+ V - carbide	2350°C: Al_4C_3

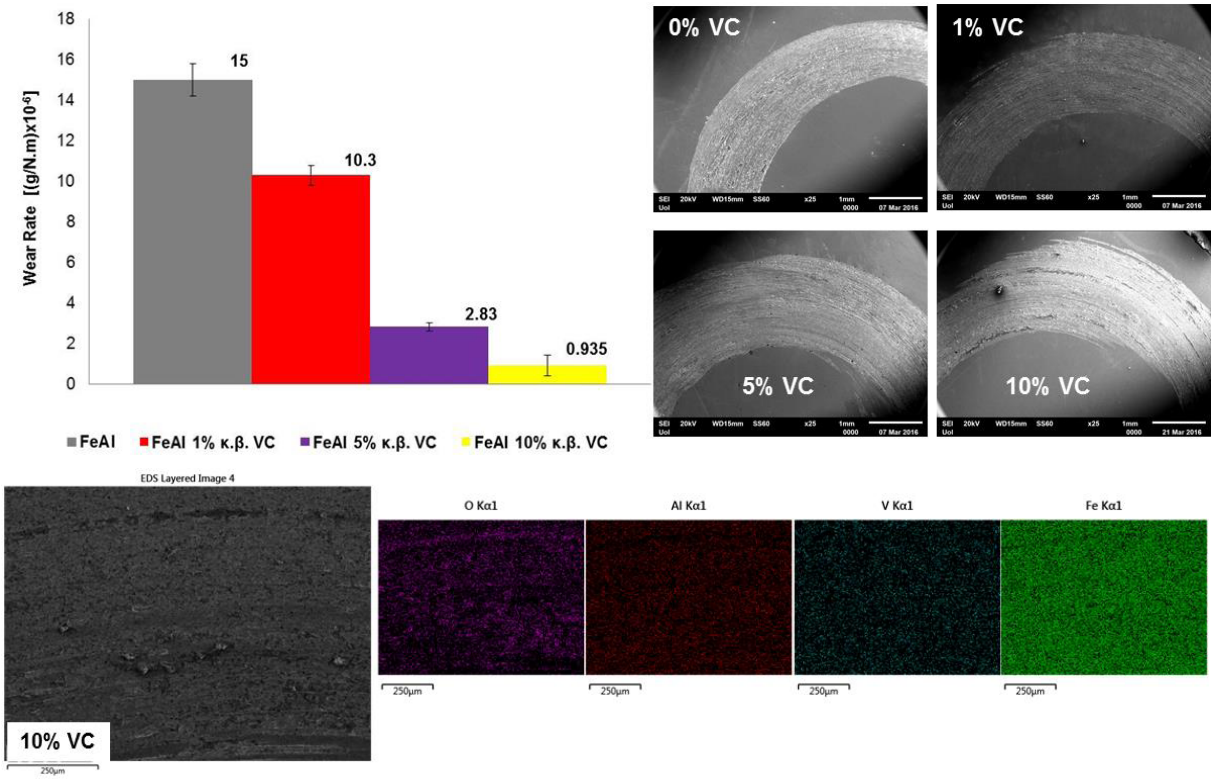

Figure 3: Sliding wear results for the different materials showing the wear rates, panoramic views of the wear tracks and EDS analysis on selective wear track area of the 5% material

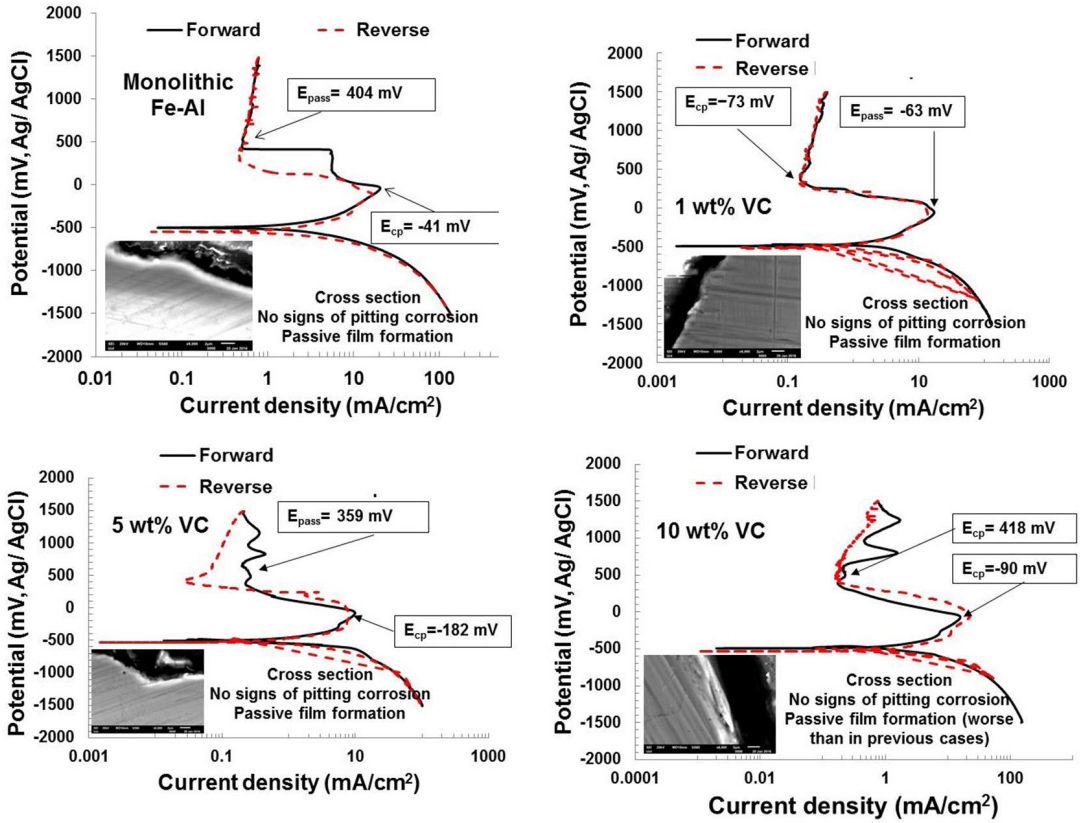

Figure 4: Cyclic potentiodynamic curves of the different materials produced at the present effort. Cross sections and major results are included

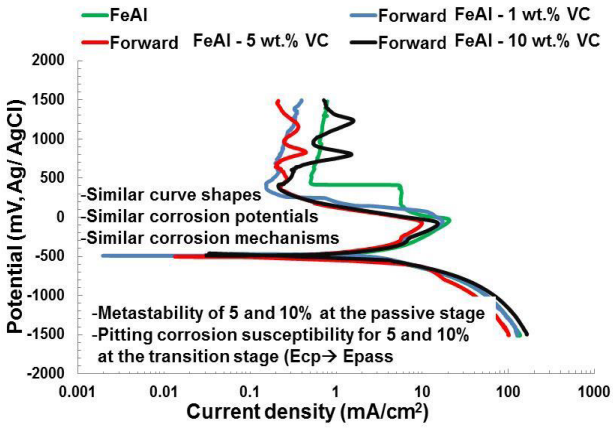

Figure 5: Forward part of the polarization curves along with the major conclusions

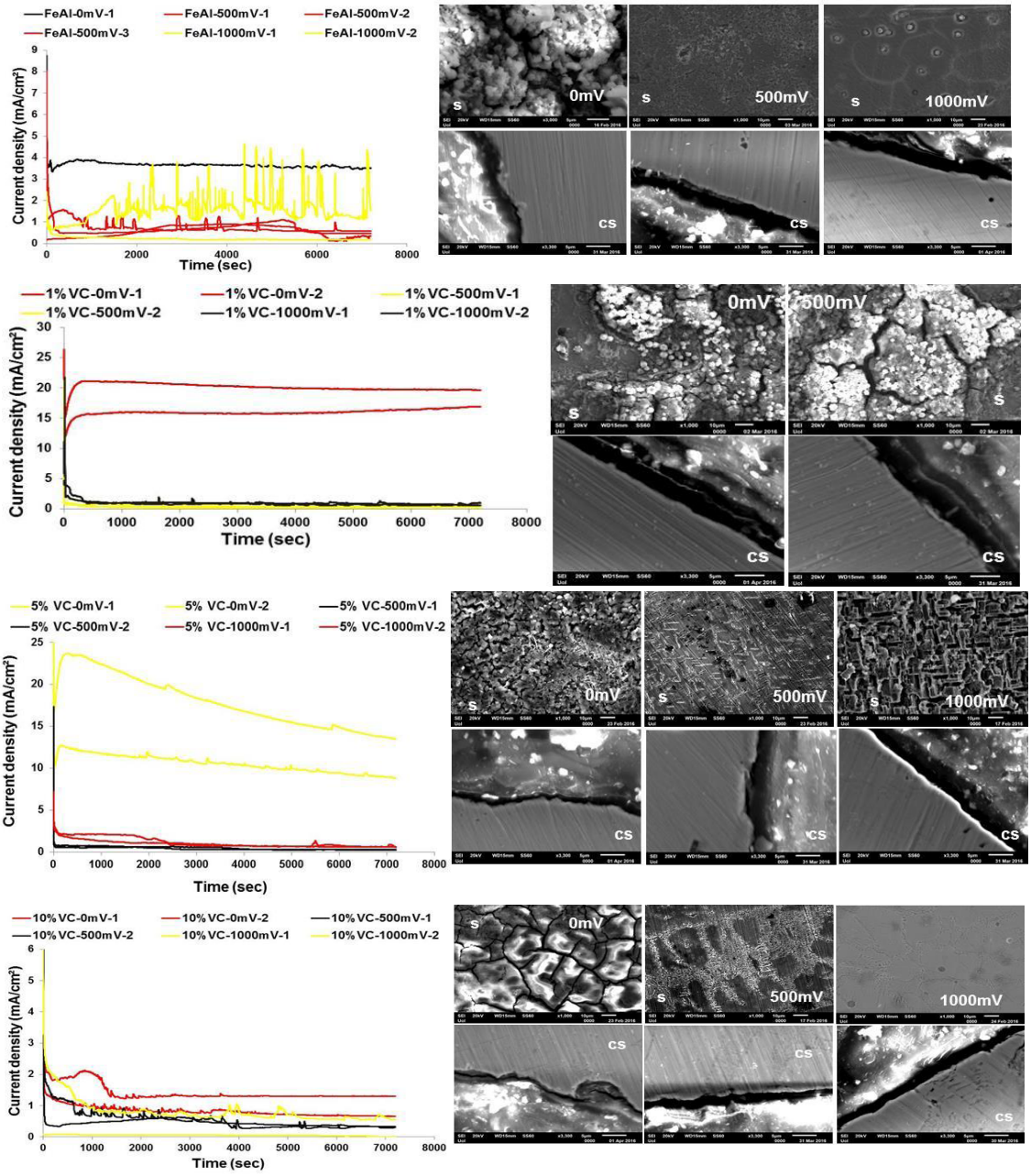

Figure 6: Chronoamperometry measurements for the different materials at different potentials. Surface (s) and cross section areas (cs) indicating the surface status after each treatment

2. The microstructure significantly alters at high VC additions, with the formation of eutectic compounds being the main features and significant alterations on the matrix compositional schemes being the main feature.
3. Sliding wear resistance was improved with addition of the VC phase.
4. Aqueous corrosion tests, showed passivation for all materials, with some metastability for the higher VC additions.

Acknowledgments

The authors would like to acknowledge Prof. S. Makridis for applying part of the arc-melting apparatus system under his patent: https://www.researchgate.net/publication/200664162_Multiapparatus_Arc_Melting_for_Rapid_Solidification_Processes?ev=prf_pub.

References

1. Stoloff NS, Liu CT, Deevi SC. Emerging applications of intermetallics. Intermetallics. 2000; 8(9-11):1313-1320. doi: http://dx.doi.org/10.1016/S0966-9795(00)00077-7.
2. Johnson DR. Intermetallic-based composites. Current opinion in solid state and materials science. 1999; 4(3):249-253. doi: http://dx.doi.org/10.1016/S1359-0286(99)00020-0.
3. Ward-Close CM, Monir R, Doorbar PJ. Intermetallic-matrix composites—a review. Intermetallics. 1996; 4(3):217-229. doi: http://dx.doi.org/10.1016/0966-9795(95)00037-2.
4. Yang J, La P, Liu W, Xue Q. Tribological properties of FeAlintermetallics under dry sliding. Wear. 2004; 257(1-2):104-109. doi: http://dx.doi.org/10.1016/j.wear.2003.10.012.
5. Qiu J, Baker I, Kennedy FE, Liu Y, Munroe PR. The effects of stoichiometry on the dry sliding wear of FeAl. Intermetallics. 2013; 40:19-27. doi: http://dx.doi.org/10.1016/j.intermet.2013.03.020.
6. Kim YS, Kim YH. Sliding wear behavior of Fe_3Al-based alloys. Materials Science and Engineering: A. 1998; 258(1-2):319-324. doi: http://dx.doi.org/10.1016/S0921-5093(98)00951-4.
7. Zhang X, Ma J, Yang J, Bi Q, Liu W. Dry-sliding tribological behavior of Fe–28Al–5Cr/TiC composites. Wear. 2011; 271(5-6):881-888. doi: http://dx.doi.org/10.1016/j.wear.2011.03.020.
8. Rao VS. A review of the electrochemical corrosion behaviour of iron aluminides. ElectrochemicaActa. 2004; 49(26):4533-4542. doi: http://dx.doi.org/10.1016/j.electacta.2004.05.033.
9. Rao VS. High temperature oxidation behaviour of Fe-Al-C alloys: An overview. Materials Science and Engineering A. 2004; 364(1):232–239. doi: http://dx.doi.org/10.1016/j.msea.2003.08.031.
10. Sharma G, Sign PR, Sharma RK, Gaonkar KB, Ramanujan RV. Aqueous Corrosion Behavior of Iron aluminideIntermetallics. Journal of Materials Engineering and Performance. 2007; 16(6):779-783. doi: http://dx.doi.org/10.1007/s11665-007-9131-2.
11. Negache M, Taibi K, Souami N, Bouchemel H, Belkada R. Effect of Cr, Nb and Zr additions on the aqueous corrosion behavior of iron-aluminide. Intermetallics. 2013; 36:73-80. doi: http://dx.doi.org/10.1016/j.intermet.2013.01.001.
12. Chen Y, Wang HM. Laser melted TiC reinforced nickel aluminide matrix in situ composites. Journal of alloys and compounds. 2005; 391(1-2):49-54. doi: http://dx.doi.org/10.1016/j.jallcom.2004.08.066.
13. Chen Y, Wang HM. Growth morphology and mechanism of primary TiC carbide in laser clad TiC/FeAl composite coating. Materials Letters. 2003; 57(5-6):1233-1238. doi: http://dx.doi.org/10.1016/S0167-577X(02)00964-3.
14. Chen Y, Wang HM. Microstructure and wear resistance of laser clad TiC reinforced FeAl intermetallic matrix composite coatings. Surface and Coatings Technology. 2003; 168(1):30-36. doi: http://dx.doi.org/10.1016/S0257-8972(02)00881-2.
15. Chen Y, Wang HM. High-temperature wear resistance of a laser clad TiC reinforced FeAl in situ composite coating. Surface and Coatings Technology. 2004; 179(2-3):252-256. doi: http://dx.doi.org/10.1016/S0257-8972(03)00821-1.
16. Chen Y, Wang HM. Eutectic MC carbide growth morphologies of a laser clad TiC/FeAl composite coating. Materials Letters. 2005; 59(28):3699-3702. doi: http://dx.doi.org/10.1016/j.matlet.2005.06.051.
17. Chen Y, Wang HM. Growth morphologies and mechanisms of non-equilibrium solidified MC carbide. Journal of Materials Research. 2006; 21(2):375-379. doi: https://doi.org/10.1557/jmr.2006.0043.
18. Wang HM, Yu LG, Li XX, Jiang P. Growth morphology and mechanism of MC carbide under quasi-rapid solidification conditions. Science and Technology of Advanced Materials. 2001; 2(1):173-176. doi: http://dx.doi.org/10.1016/S1468-6996(01)00044-4.
19. Chen Y, Wang HM. Growth morphologies and mechanism of TiC in the laser surface alloyed coating on the substrate of TiAlintermetallics. Journal of Alloys and Compounds. 2003; 351(1-2):304-308. doi: http://dx.doi.org/10.1016/S0925-8388(02)01077-0.
20. Chen Y, Wang HM. Rapidly solidified MC carbide morphologies of a pulsed laser surface alloyed γ-TiAl intermetallic with carbon. ScriptaMaterialia. 2004; 50(4):507-510. doi: http://dx.doi.org/10.1016/j.scriptamat.2003.10.028.
21. Chen Y, Wang HM. Microstructure and wear resistance of laser-melted TiC reinforced nickel aluminide dual-phase matrix in situ composite. Intermetallics. 2006; 14(3):325-331. doi: http://dx.doi.org/10.1016/j.intermet.2005.06.011.
22. Karantzalis AE, Lekatou A, Georgatis M, Arni Z, Dracopoulos V. Solidification observations of vacuum arc melting processed Fe–Al–TiC composites: TiC precipitation mechanisms. Materials Characterization. 2011; 62(12):1196-1204. doi: http://dx.doi.org/10.1016/j.matchar.2011.10.009.
23. Velon A, Olefjord I. Oxidation Behavior of Ni_3Al and Fe_3Al: I. XPS Calibrations of Pure Compounds and Quantification of the Results. Oxidation of Metals. 2001; 56(5):415–424. doi: http://dx.doi.org/10.1023/A:1012589315800.
24. Gesmundo F, Gleeson B. Oxidation of multicomponent two-phase alloys. Oxidation of Metals. 1995; 44(1):211–237. doi: http://dx.doi.org/10.1007/BF01046728.
25. Archard JF. Contact and Rubbing of Flat Surfaces. Journal of Applied Physics. 1953; 24(8):981–988. doi: http://dx.doi.org/10.1063/1.1721448.
26. Mavros H, Karantzalis AE, Lekatou A. Solidification observations and sliding wear behavior of cast TiC particulate-reinforced AlMgSi matrix composites. Journal of Composite Materials. 2012; 47(17):2149–2162. doi: https://doi.org/10.1177/0021998312454901.
27. Kim YS, Kim YH. Sliding wear behavior of Fe_3Al-based alloys, Materials Science and Engineering: A. 1998; 258(1-2):319-324. doi: http://dx.doi.org/10.1016/S0921-5093(98)00951-4.